J|A|C|S JOURNAL OF THE AMERICAN CHEMICAL SOCIETY

Article

pubs.acs.org/JACS

SERS-Fluorescence Joint Spectral Encoding Using Organic–Metal–QD Hybrid Nanoparticles with a Huge Encoding Capacity for High-Throughput Biodetection: Putting Theory into Practice

Zhuyuan Wang, Shenfei Zong, Wang Li, Chunlei Wang, Shuhong Xu, Hui Chen, and Yiping Cui*

Advanced Photonics Center, School of Electronic Science and Engineering, Southeast University, Nanjing 210096, China

Supporting Information

ABSTRACT: A new concept of optical encoding approach, surface enhanced Raman scattering (SERS)-fluorescence joint spectral encoding method (SFJSE), was demonstrated by using organic–metal–quantum dot (QD) hybrid nanoparticles (OMQ NPs) with a nanolayered structure. This method has two distinct characteristics, which make it more feasible to achieve enormous codes in practice, compared with a sole fluorescence- or SERS-based encoding protocol. One of the two characteristics is to use the joint SERS and fluorescence spectra as the encoding elements instead of an individual optical signal, resulting in a broadened optical spectrum range for efficient encoding. The other is to assemble SERS reporters and fluorescent agents onto different layers of OMQ NPs, leading to an easier fabrication protocol when a large number of agents need to be involved into encoding carriers. By conjugating different antibodies to OMQ NPs with varied codes, the potential application of such an encoding system in high-throughput detection has been investigated by multiplex sandwich immunoassays. The high specificity and sensitivity of the assays suggest that the SFJSE method could be developed as a powerful encoding tool for high-throughput bioanalysis with the use of OMQ NPs.

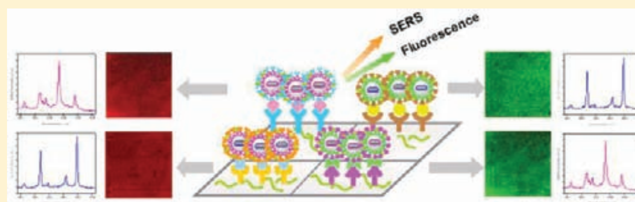

INTRODUCTION

High-throughput sensing technologies have become increasingly important with the growing demands for molecular biology analysis, disease diagnosis, and drug discovery.[1] One of the most popular ways for a multiplex assay is to use the encoding microbeads or nanoprobes with a unique code to identify the attached ligand molecules.[2] Although fluorescence- and SERS-based encoding protocols show particular promise for multiplex detection,[3] the amount of acquired molecular information is restricted by the number of distinguishable codes in the same array. In principle, the narrow emission spectra from semiconductor quantum dots (QDs), one of the representative fluorescent encoding materials, allow 10–12 different colors to be resolved in the visible region (380–780 nm) with acceptable spectral overlap.[1] However, the number of spectrally distinct codes that can be generated is limited practically due to the complicated process, such as fluorescence resonance energy transfer between QDs with overlapping excitation and emission spectra. So far, QDs with 2–4 different emission wavelengths have been mostly employed for encoding,[4] which means that only a limited part of the fluorescence emission spectral region has been employed. Similarly, in a SERS-based encoding system, the number of the codes that can be realized experimentally is also restricted by several problems. Specifically, the Raman fingerprint regions of most organic SERS reporters are in the range 500–2000 cm^{-1} (i.e., only ~100 nm for excitation wavelengths at visible region), and the commonly used SERS reporters have similar chemical structures. Therefore, decoding the Raman spectrum of a plurality of reporters may become difficult owing to the spectral overlap.[5] On the other hand, since the encoded carriers are usually fabricated by the incorporation of different agents with distinguishable ratios, the amounts of various encoding agents must be controlled precisely during the preparation.[6] Thus, with the increasing number of involved agents, the preparation process of encoded carriers may become rather difficult and time-consuming, especially when large numbers of the agents are assembled onto the same layer of the nano- or microsized spherical supports. All of these factors restrict the number of codes that can be realized practically, which is far less than that predicted theoretically.[1] Therefore, a novel encoding method with an increased encoding capability is still required for the easy and rapid identification of large chemical and biological libraries.

Herein, we propose the use of SERS-fluorescence joint spectra to develop a new encoding approach (denoted as SFJSE) based on organic–metal–QD hybrid nanoparticles with a nanolayered structure (denoted as OMQ NPs). This method has two characteristics to ensure a greatly enlarged encoding capacity. First, by using joint SERS-fluorescence signals as the encoding elements, the spectral range available for encoding is broadened because of the utilization of both photoluminescence (PL) and SERS spectral regions, allowing for more spectrally distinguishable codes. Moreover, the number of available codes can be further increased when the

Received: August 29, 2011
Published: January 9, 2012

 © 2012 American Chemical Society

intensity encoding mode is also considered. Second, in such OMQ NPs, SERS and fluorescent agents are assembled onto two different layers. It makes the fabrication process easier and more controllable for increasing the number of involved agents. Therefore, using the proposed SFJSE method, the number of the codes that can be generated practically is much more than that through a traditional fluorescence- or SERS-based encoding method (denoted as FE and SE, respectively), which makes the SFJSE approach particularly promising for multiplex bioanalysis at high levels. As a proof-in-principle experiment, the application of encoded OMQ NPs in protein detection is demonstrated using multiplex sandwich immunoassays. The distinct and strong optical signals of antibody-conjugated OMQ NPs afford protein detection sensitivity down to 1 fM with a large dynamic range.

■ RESULTS AND DISCUSSION

Synthesis of OMQ NPs. Recently, increasing attention has been paid to the fabrication of hybrid nanoparticles for research and clinical applications.[7] Interestingly, by incorporating both organic dyes and Au nanoparticles inside a nanocomposite sphere, a novel kind of probe for multimode imaging has been developed by Ren's group and our previous work based on fluorescence and SERS signals.[8] More recently, using CdTe QDs as the fluorescent indicators, we described a type of composite nanoparticles as 4-mercaptobenzoic acid (4MBA)−gold aggregates−CdTe for cellular imaging, which exhibits switchable fluorescence and SERS signals.[9] Here, as a model study, we synthesized the OMQ NPs comprising of SERS reporters-functionalized Au@Ag nanorods (NRs) and CdTe QDs, which were employed as the encoding carriers exhibiting both fluorescence and SERS signals. Scheme 1 shows the fabrication procedure of such a hybrid nanoparticle, which comprises a SERS reporters-functionalized Au@Ag NR core, an intermediate layer of silica, and an outer shell of CdTe QDs. The presented nanoparticles were fabricated through three main steps. First, Au@Ag NRs were obtained by depositing a Ag shell on CTAB-stabilized Au NRs through a modified method developed by Xiang et al..[10] Second, the solution of Au@Ag NRs was mixed with SERS reporters, followed by the encapsulation of a silica shell through a modified Stöber method.[11] Finally, after the silica nanoparticles were modified with amino groups, a dense monolayer of CdTe QDs was chemically attached onto their surfaces by using 1-ethyl-3-(3-dimethylaminopropyl) carbodiimide (EDC) and *N*-hydroxysuccinimide (NHS). In such a system, although Au NRs can be used as the cores directly, Au@Ag NRs were fabricated here for achieving a much stronger SERS signal, which is advantageous for improving the sensitivity of an encoding system.

Scheme 1. Preparation of Organic−Metal−QD Hybrid Nanoparticles (OMQ NPs)

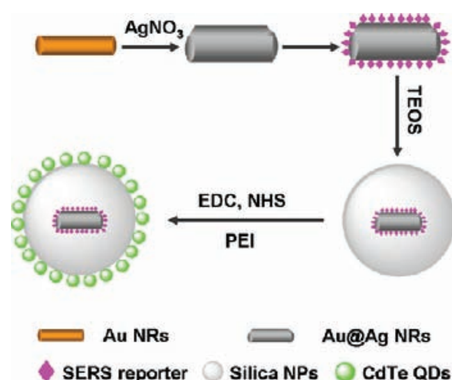

The initial Au NRs were prepared through the seed-mediated growth procedure, and the aspect ratio was about 3.2 (Figure 1A).

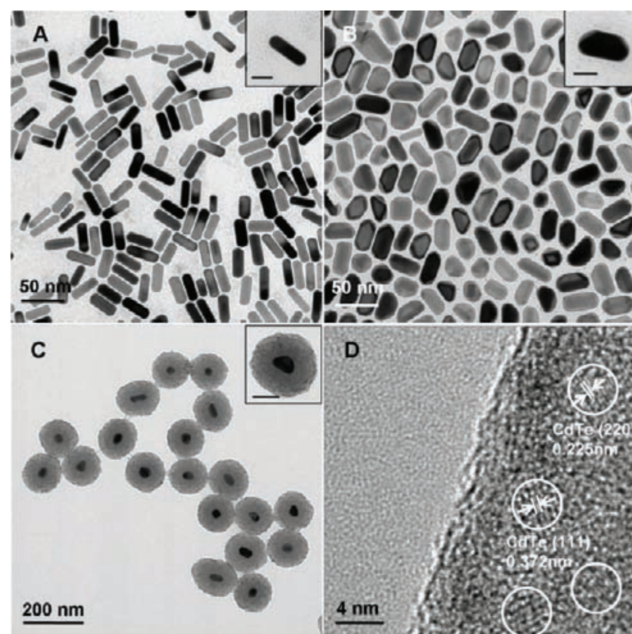

Figure 1. TEM images of (A) Au NRs, (B) Au@Ag NRs, and (C) OMQ NPs. The insets in parts A−C show the enlarged individual Au NR, Au@Ag NR, and OMQ NP, respectively. The scale bars in the three insets are 20, 20, and 50 nm, respectively. (D) HRTEM image of CdTe QDs adsorbed on the surface of an OMQ NP. The white circle indicates a single CdTe QD.

After being deposited with Ag shell, the resulting Au@Ag bimetallic nanorod shows an "orange slice-like" shape due to the anisotropic Ag coating (Figure 1B), agreeing quite well with the previously reported results.[10] Figure 2 shows the extinction spectra of the as-prepared Au NRs and Au@Ag NRs. The Au NRs show a longitudinal SPR peak at 675 nm and a transverse one at 516 nm. After being coated with Ag shell, the longer SPR wavelength hypsochromically shifted to 537 nm. In the short wavelength region, there are two new bands centered at 347 and 390 nm, which might indicate the unsymmetrical structure of the deposited Ag shell.[10] Besides, the color of the Au NRs solution is blue while that of Au@Ag NRs is rose (Figure 2, inset).

The as-prepared Au@Ag NRs were then mixed with the proper SERS reporters for generating SERS signals, followed by being encapsulated with a layer of silica through a modified Stöber-based synthesis method.[11] The surfaces of the resulting silica nanoparticles were then modified with amino groups by being mixed with poly(ethyleneimine) (PEI) solution. Finally, the surface-modified silica cores were conjugated with thioglycolic acid (TGA)-capped CdTe QDs using EDC and NHS as zero-length cross-linkers. By using such a structure, SERS reporters and fluorescent agents were assembled onto two different layers of OMQ NPs. Figure 1C shows a typical TEM image of the hybrid OMQ nanospheres. It reveals that the thickness of silica shell is about 40 nm and many CdTe QDs exist on the surface of each silica core. Moreover, the high-resolution TEM (HRTEM) image shown in Figure 1D exhibits

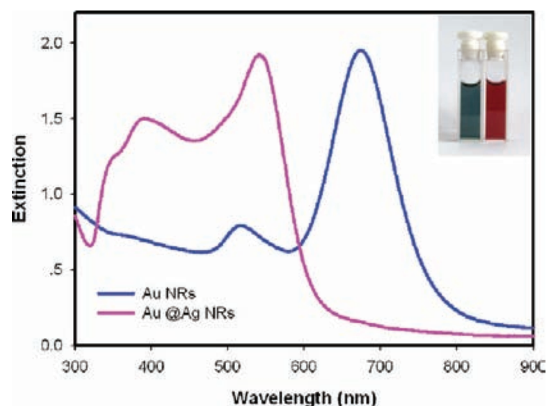

Figure 2. Extinction spectra of Au NRs and Au@Ag NRs. The inset shows the photograph of Au NRs (left) and Au@Ag NRs (right).

the clear lattice spacings of 3.72 and 2.25 Å for the QDs on the surfaces of silica nanoparticles, which are attributed to the (111) and (220) planes of cubic (zinc blende) CdTe. These results confirm that CdTe QDs have been successfully conjugated onto the surfaces of silica nanoparticles. The growth of silver on Au NRs and the capture of CdTe QDs on the silica nanoparticles have also been verified by X-ray photoelectron spectroscopy (XPS) (Figure S1). Further, the structural features of the OMQ nanocomposites have been confirmed by using the scanning transmission electron microscopy (STEM) imaging and energy dispersive X-ray (EDX) elemental mapping of OMQ spheres (Figure 3). The strong Ag signal surrounding the Au NRs confirms the Au@Ag NRs core, while the Cd signals detected in the surface region clearly suggest the conjugation of CdTe QDs on silica nanoparicles.

Fluorescence and SERS Characterizations of OMQ NPs. In such OMQ NPs, fluorescence and SERS signals can be separately generated by using different excitation wavelengths. Here, excitation wavelength at 400 nm was selected to generate fluorescence while that at 633 nm was used to obtain SERS signals. As an example to illuminate the application of the nanospheres as encoded carriers in an SFJSE system, CdTe QDs with 2 different emission wavelengths and 2 SERS reporters were employed as the encoding agents. They are CdTe QDs with an emission peak at 515 nm (denoted as CdTe 515), CdTe QDs with an emission peak at 591 nm (denoted as CdTe 591), 4-mercaptobenzoic acid (4MBA), and 5,5′-dithiobis-(2-nitrobenzoic acid) (DTNB), respectively. Figure 4A shows

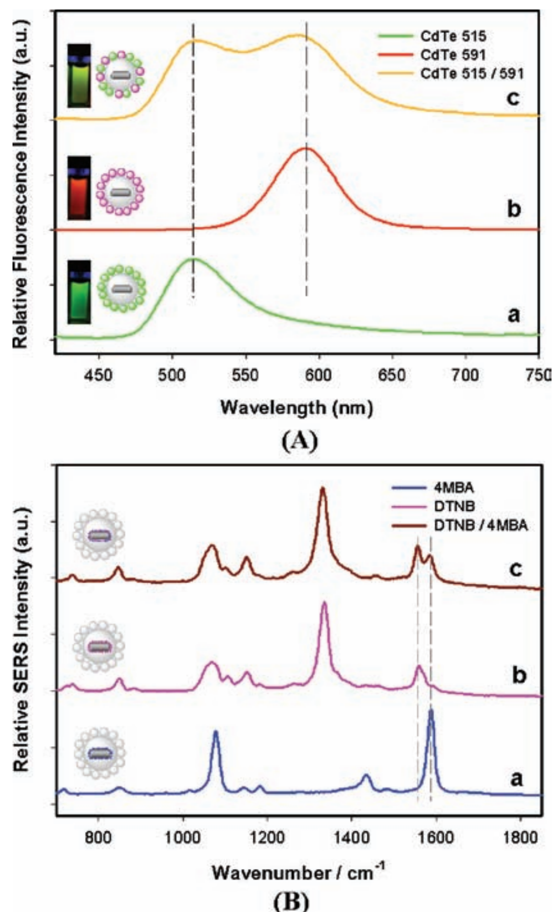

Figure 4. (A) PL and (B) SERS spectra of the composite nanoparticles using CdTe 515, CdTe 591, and CdTe 515/591 (volume ratio is 9:1) as the fluorescence indicators and 4MBA, DTNB, 4MBA/DTNB (molar ratio is 5:2) as the SERS reporters.

the PL spectra of silica nanoparticles conjugated with CdTe 515, CdTe 591, and the mixture of both with a volume ratio of

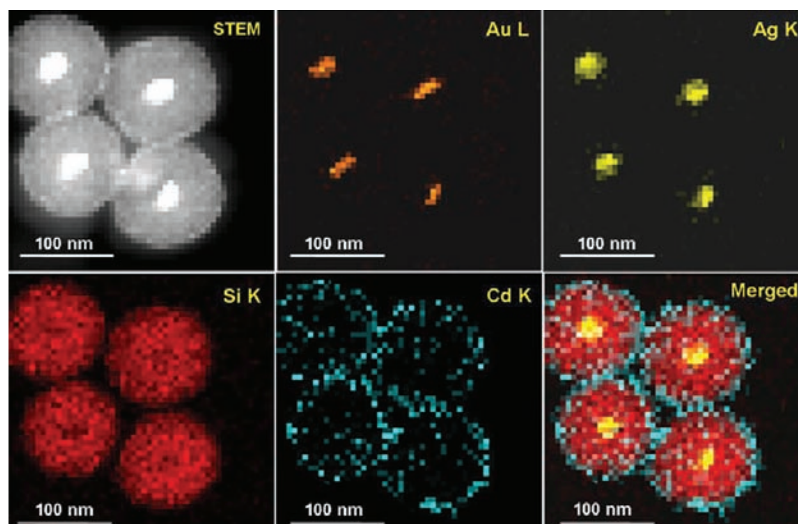

Figure 3. STEM image and the corresponding EDX elemental distribution of Au, Ag, Si, Cd in OMQ NPs. The merged mapping is also shown.

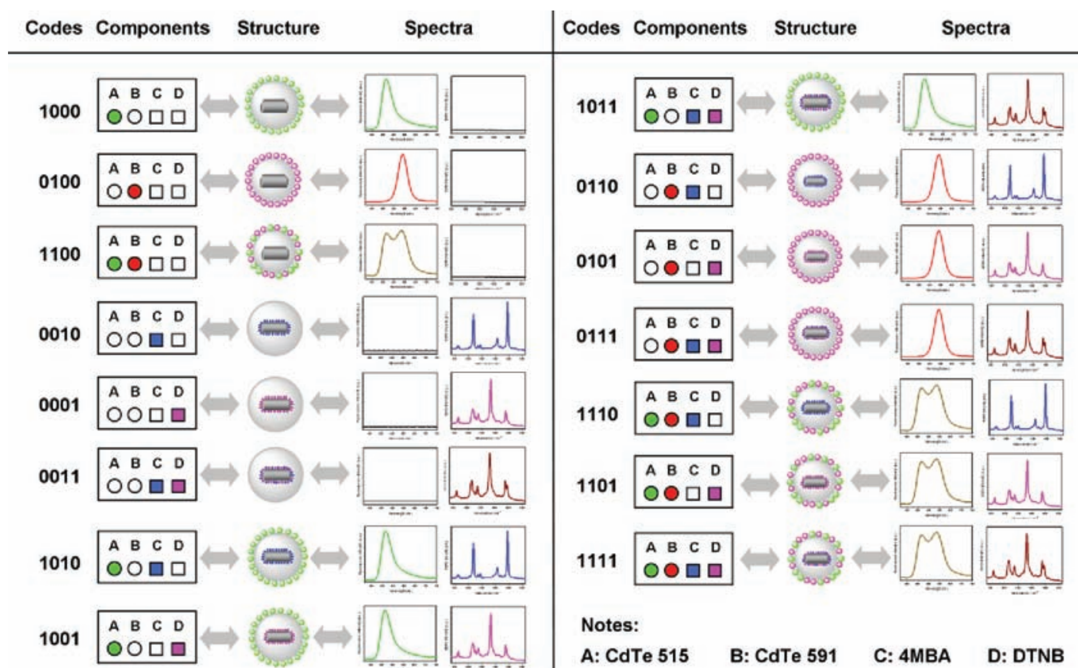

Figure 5. Composition, measured spectra, and codes of the synthesized 15 nanoparticles.

Scheme 2. Schematic Illustration of Multianalyte Immunoassay Based on the Synthesized Encoding Carriers Using a Sandwich Structure Concept

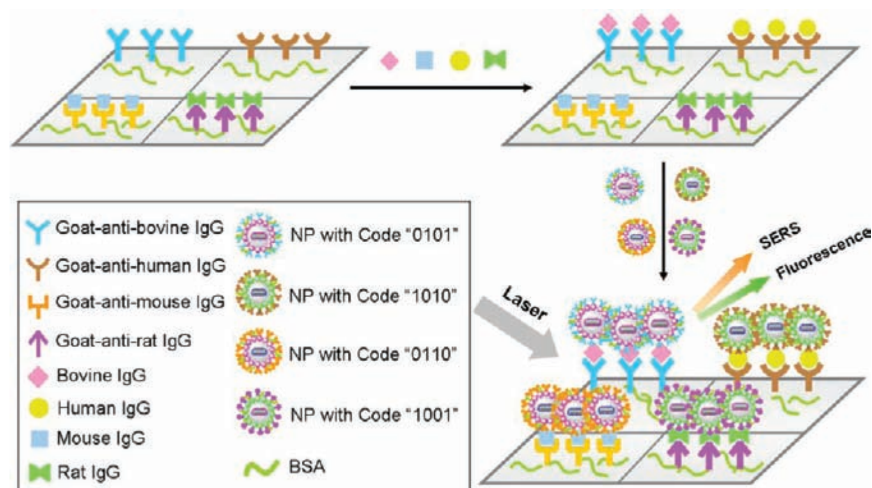

9:1 (denoted as CdTe 515/591), respectively. It can be clearly observed that the silica NPs with CdTe 515/591 exhibit a well-resolved dual fluorescence emission, indicating that the multicolor encoding fluorescent spheres can be generated using this composite structure.

The SERS spectra of the hybrid nanoparticles containing 4MBA, DTNB, and the mixture are shown in Figure 4B. The SERS characteristics of the reporters retained quite well after being incorporated inside silica shells coated with CdTe QDs. The SERS spectrum of 4MBA is dominated by peaks at 1077, 1590, and 1434 cm^{-1} while that of DTNB is characterized by peaks at 1333, 1067, 1152, and 1558 cm^{-1}. When the mixture of 4MBA and DTNB with a molar ratio of 5:2 was used as the SERS agent, signal peaks at 1558 and 1590 cm^{-1} can be observed simultaneously.

Encoding Capacity of OMQ NPs Using SFJSE Method. On the basis of the above combination of fluorescent and SERS agents, a total of 15 codes were achieved experimentally with distinguished optical spectral signals, whose components, structures, and measured optical spectra are listed in Figure 5. However, in a traditional FE or SE encoding system, only 3 codes can be generated using those 2 fluorescence or 2 SERS agents. Definitely, many other QDs and SERS-label molecules can be used in SFJSE encoding systems with strong fluorescence and SERS signatures. Therefore, the potential number of codes N can be increased simply by increasing the number of different QDs and SERS agents, which can be expressed with a simple combination calculus with repetition as follows:

$$N = \sum_{i=1}^{m+n} C_{m+n}^{i} = \sum_{i=1}^{m+n} \frac{(m+n)!}{i!(m+n-i)!} = 2^{m+n} - 1 \quad (1)$$

$$N/N_1 = (2^{m+n} - 1)/(2^{m} - 1),$$
$$N/N_2 = (2^{m+n} - 1)/(2^{n} - 1) \quad (2)$$

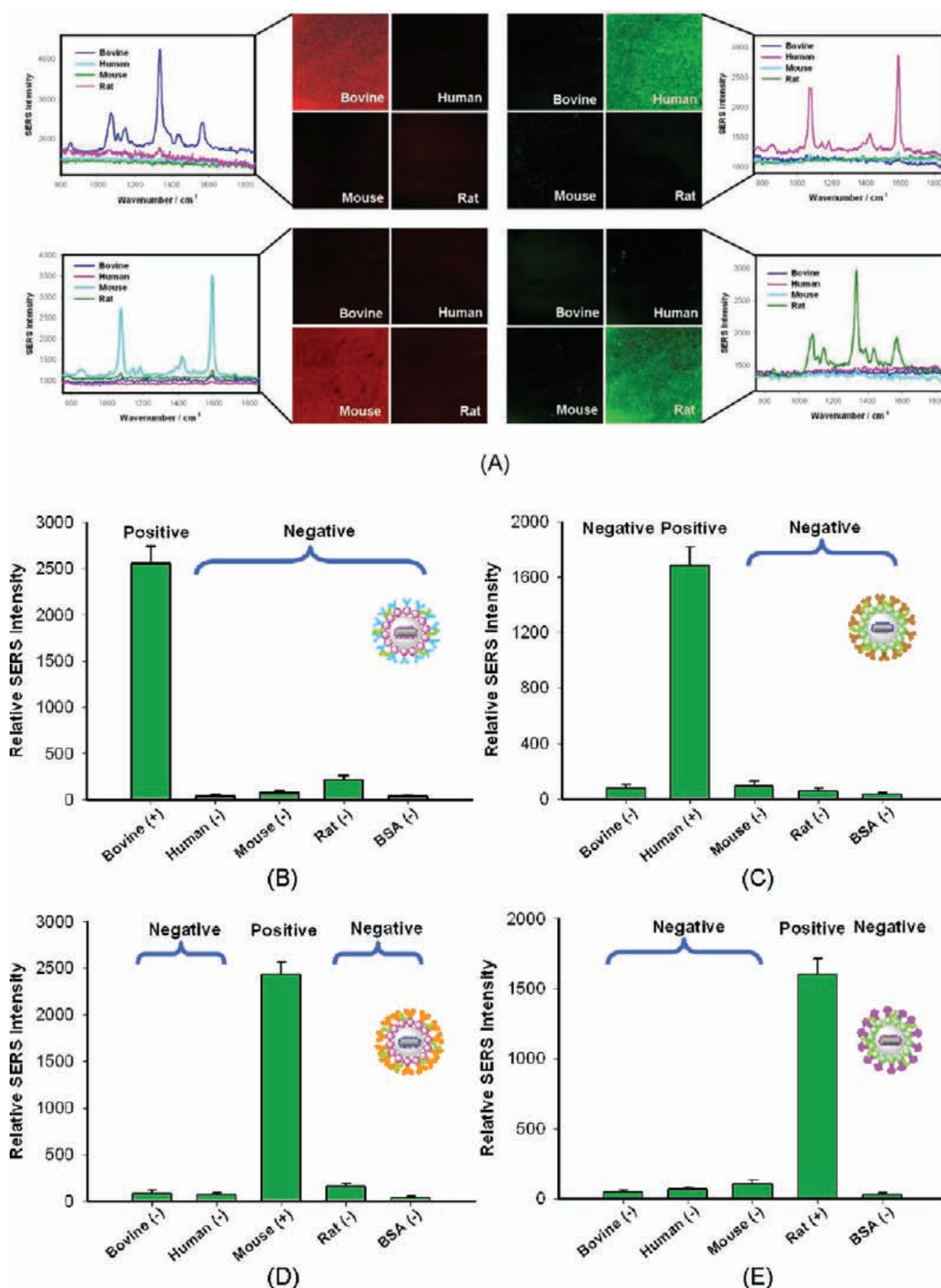

Figure 6. (A) Fluorescence images and SERS spectra of four sandwiched assays, which were pipetted with goat-antibovine IgG-modified 0101 code (top-left), goat-antihuman IgG-modified 1010 code (top-right), goat-antimouse IgG-modified 0110 code (bottom-left), and goat-antirat IgG-modified 1001 code (bottom-right), respectively. (B−E) Histogram illustrating the different SERS intensities at 1333 cm^{-1} (for DTNB) or 1590 cm^{-1} (for 4MBA) in four sandwiched assays, which were pipetted with (B) goat-antibovine IgG-modified 0101 code, (C) goat-antihuman IgG-modified 1010 code, (D) goat-antimouse IgG-modified 0110 code, and (E) goat-antirat IgG-modified 1001 code, respectively. Error bars indicate the standard deviations from 12 measurements. BSA was used as a negative control in all four assays. Intensities shown are after the subtraction of background.

where N is the total possible number of codes using SFJSE, m is the number of QDs fluorophores, and n is the number of SERS reporters. $N_1 = 2^m - 1$ and $N_2 = 2^n - 1$ are the numbers of codes in FE and SE encoding systems, respectively. From these equations, the greatly enlarged encoding capacity of SFJSE method can be clearly demonstrated. For example, for $m = 5$ and $n = 5$, N is 1023 while only 31 codes can be obtained based on a sole fluorescence or SERS method.

Although, in principle, the same amount of codes can be obtained by using $m + n$ kinds of agents in an FE or SE system, the preparation process will become rather complicated or even unpractical because of the problems of spectral overlap or limited available types of agents, especially when the value of $m + n$ is large. However, in the SFJSE approach, enlarging the number of codes is much easier and more feasible due to the following two reasons. First, by using the combined

dx.doi.org/10.1021/ja208154m | J. Am. Chem.Soc. 2012, 134, 2993−3000

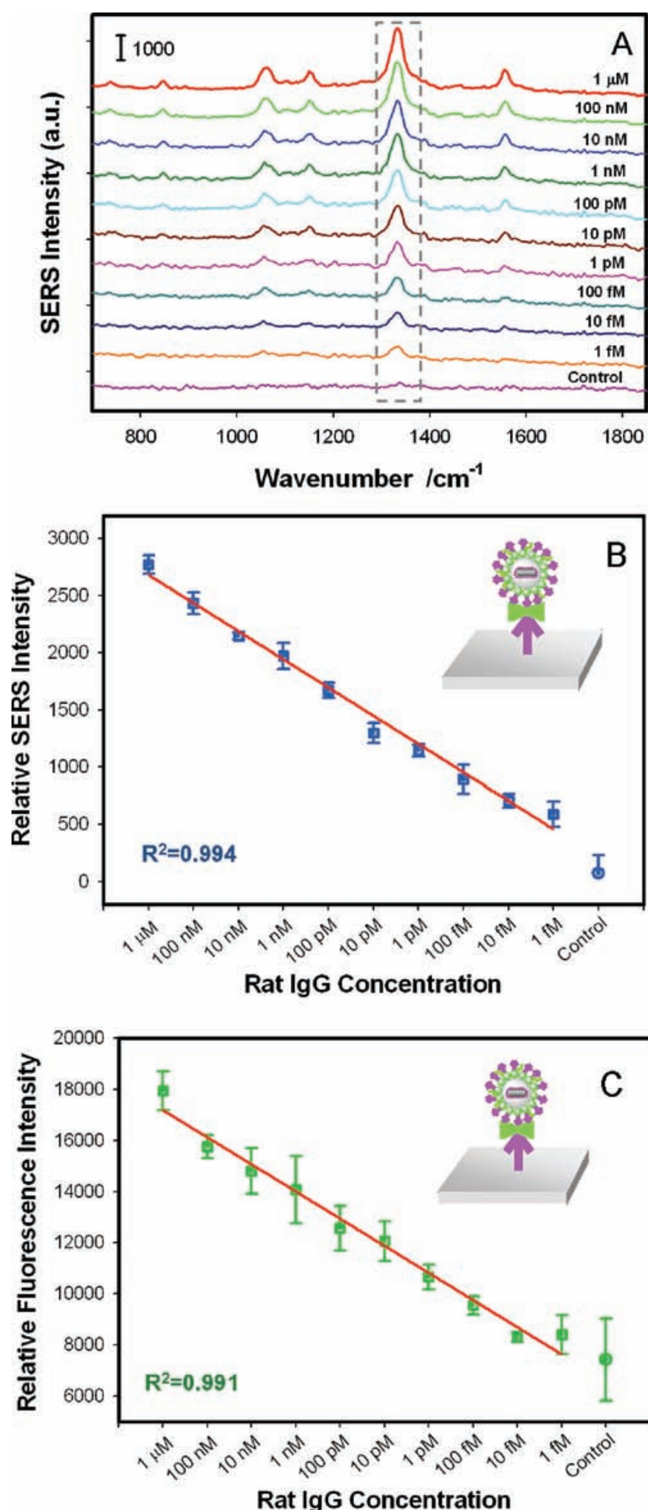

Figure 7. (A) Concentration-dependent SERS spectra for rat IgG detection using goat-antirat IgG-modified 1001 code. The concentration of rat IgG ranged from 1 μM to 1 fM. The control spectrum was obtained by replacing rat IgG with BSA in the sandwich immunoassay. (B) Plot of SERS intensity at peak 1333 cm^{-1} as a function of the logarithm of rat IgG concentration. Error bars indicate the standard deviations from 12 measurements. Intensities shown are after background subtraction. (C) Mean fluorescence as a function of the logarithm of rat IgG concentration from 1 μM to 1 fM. Error bars indicate the standard deviations from 12 measurements. The control spectrum was obtained by replacing rat IgG with BSA in the sandwich immunoassay.

fluorescence and SERS spectra, the efficient spectrum range for encoding in SFJSE is broader than that in an FE or SE system. Additionally, there is no energy transfer between fluorescence and SERS signals. Thus, the problem of spectral overlap is alleviated, allowing for more spectrally distinct codes. Second, the m kinds of fluorescent agents and n types of SERS reporters are conjugated onto two different layers in OMQ NPs, which is a much simpler and more controllable process compared with that to assemble $m + n$ kinds of agents in one layer. Therefore, the number of available codes can be greatly enlarged not only in theory but also in practice when the SFJSE method is used.

Another thing worth noting is that presently existing optical encoding methods are based on two main modes. One is wavelength encoding mode and the other is intensity encoding mode.[1,3b] The above calculated number in eq 1 is acquired only according to the wavelength encoding mode. Actually, a much larger number of codes will be generated when intensity encoding mode is also considered, which can be realized by controlling the amount of each optical agents in the carriers.

Selective and Sensitive Protein Detection by OMQ NPs. Further, to demonstrate the reliability of OMQ NPs as encoded carriers in multiplex immunoassays, four kinds of NPs with codes as 1001, 1010, 0110, 0101 were chosen as the models in a sandwiched immunoassay structure, which were modified with goat-antirat IgG, goat-antihuman IgG, goat-antimouse IgG, and goat-antibovine IgG, respectively (Scheme 2). Carboxylic acid groups of TGA on the CdTe QD surfaces were conjugated with the amine groups of proteins using EDC and NHS as cross-linking reagents. The empty sites on the nanospheres were blocked with bovine serum albumin (BSA) to avoid undesired adsorption. In a typical experiment, goat-antirat IgG, goat-antihuman IgG, goat-antimouse IgG, and goat-antibovine IgG were immobilized on four different spots in a chip, followed by the interaction with an analyte containing mixed human IgG, bovine IgG, rat IgG, and mouse IgG antigens. Then, the prefunctionalized carriers with codes 1001, 1010, 0110, and 0101 were pipetted onto four such chips for analysis, and each chip was incubated with one kind of code carrier for checking the specificity. After the reaction, the chips were washed with phosphate buffered saline Tween-20 (PBST) and phosphate buffered saline (PBS) to remove the unbound analytes. For each chip fluorescence images and SERS spectra were obtained using excitation wavelengths of 458 and 633 nm, respectively. It can be seen that strong fluorescence and SERS signals with specific spectra were observed only at the regions immobilized with the corresponding antigens, showing high specificities (Figure 6A). The SERS intensities obtained in those four sandwiched assays also proved that the OMQ NPs conjugated with specific antibodies bound only to the corresponding positive antigens immobilized on the substrate, and not to the other four negative-control protein spots (Figure 6B–E, BSA was used as an additional negative control in all four assays). This proof-in-concept study demonstrates the potential utility of such OMQ NPs encoded by the SFJSE method in multiplex biological analysis.

Once the antibody-conjugated OMQ NPs were determined to be capable of detecting the antigens, the sensitivity limit of protein detection was investigated using SERS signals as well as fluorescence. In the experiments, goat-antirat IgG and goat-antirat IgG-modified 1001 code were used as the model capture and reporting agents for the detection of rat IgG in a sandwiched assay. Serial dilutions of rat IgG with the concentration ranging from 1 μM to 1 fM were placed onto

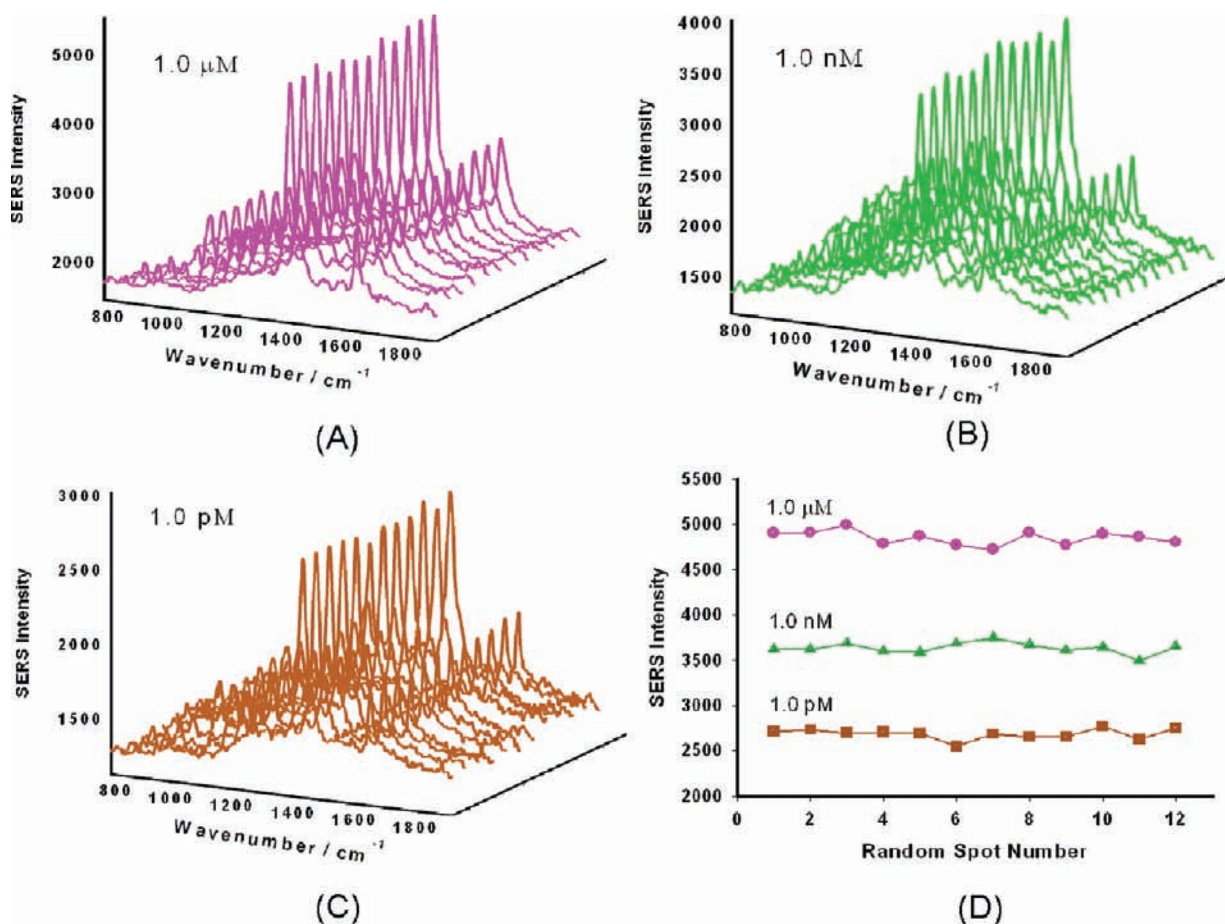

Figure 8. (A−C) SERS spectra for rat IgG detection using goat-antirat IgG-modified 1001 code measured at 12 random spots in one address on three assay chips showing the uniformity of the signal in each address. Each chip was exposed to a different concentration of rat IgG, which are (A) 1.0 μM, (B) 1.0 nM, and (C) 1.0 pM, respectively. (D) Plots of the SERS intensities at 1333 cm^{-1} from 12 random spots in one address on three assays.

the goat-antirat IgG incubated slides and then exposed to goat-antirat IgG-modified 1001 code probe (inset of Figure 7B). The concentration-dependent SERS spectra are shown in Figure 7A. It can be observed that the intensity of SERS peaks from DTNB molecules in 1001 code increased concomitantly with the increasing concentration of the antigen. For a more quantitative investigation, the results were further analyzed by plotting the intensity at 1333 cm^{-1} as a function of the logarithm of rat IgG concentration, generating the response curve in Figure 7B. The error bars indicate the standard deviations from 12 measurements. As shown in the figure, a good linear response was achieved in the concentration range from 1 μM to 1 fM. The linear regression equation is $y = -247.7x + 4162.2$, and the correlation coefficient (R^2) is 0.994. The control spectrum was obtained by replacing the target antigen with BSA in the detection system. A weak peak at 1333 cm^{-1} can be observed, indicating that there existed some nonspecific binding between the OMQ NPs and the immuno-substrate. Defining the limit of detection (LOD) as the analyte concentration that produces a signal three times larger than the standard deviation of a control measurement (without analyte),[12] the antigen detection sensitivity was reproducibly obtained as down to 1 fM, over a large dynamic range of 10 orders. On the other hand, the fluorescence intensity of CdTe QDs was also proportional to the analyte concentration in the range of 1 μM to 1 fM (Figure 7C). The linear regression equation is $y = -1062.3x + 23\,564.7$, and the correlation coefficient (R^2) is 0.991. These data indicate that highly sensitive immunoassays are possible using the OMQ NPs for quantitative detection of biomolecules.

To explore the homogeneity of the SERS signal in the immuno-assay, SERS spectra were measured at 12 randomly selected spots in one address on three chips for rat IgG detection using goat-antirat IgG-modified 1001 code. The chips were exposed to rat IgG concentration of 1.0 μM, 1.0 nM, and 1.0 pM, respectively. A good reproducibility was observed for all three chips (Figure 8A−C), which was presented more clearly in Figure 8D. For the vibration mode at 1333 cm^{-1}, the relative standard deviations of the intensity were 5.6%, 6.9%, and 8.2% for the above concentrations, respectively.

■ CONCLUSIONS

In conclusion, a new encoding method, SFJSE, based on a joint SERS-fluorescence spectrum, has been proposed using OMQ NPs. When m kinds of QDs and n kinds of SERS reporters are employed, the number of available codes dramatically increases to $(2^{m+n} - 1)$, which is $((2^{m+n} - 1)/(2^m - 1))$ or $((2^{m+n} - 1)/(2^n - 1))$ times that obtained by using sole fluorescence or SERS spectra. Moreover, substantially more codes can be acquired when an intensity encoding mode is also used, which can be generated by controlling the concentration or ratio of each agent. Two distinct features of the SFJSE method are the

broadened spectrum range for efficient encoding and the unique structure of assembling fluorescent and SERS agents into different layers, which allow this new method to have a huge encoding capacity, not only in theory, but more importantly, in practice. After being conjugated with the specific antibodies, the OMQ NPs can be used as the encoded carriers for the detection of multiplex biomolecular analysis. The distinct and strong optical signals of our proposed OMQ NPs enable the reproducible protein detection with a large dynamic range over 10 orders and a high sensitivity down to 1 fM of analyte. The application of such OMQ NPs tags encoded by the SFJSE method in biomolecular detection is highly generalizable to any system with adequate binding affinity and specificity. We anticipate that this technology may open a new way in optical encoding systems, which could have enormous potential applications in high-throughout bioanalysis where multiplexing at high levels is needed.

■ ASSOCIATED CONTENT

Ⓢ Supporting Information

Experimental procedures and XPS spectra of Au NRs, Au@Ag NRs, silica encapsulated Au@Ag NRs, and OMQ NPs. This material is available free of charge via the Internet at http://pubs.acs.org.

■ AUTHOR INFORMATION

Corresponding Author

cyp@seu.edu.cn

■ ACKNOWLEDGMENTS

This research was supported by National Science Foundation of China (Grants 60708024, 60877024, 61177033) and Specialized Research Fund for the Doctoral Program of Higher Education (SRFDP) (Nos. 20070286058, 20090092110015).

■ REFERENCES

(1) Wilson, R.; Cossins, A. R.; Spiller, D. G. *Angew. Chem., Int. Ed.* **2006**, *45*, 6104.

(2) Han, M.; Gao, X.; Su, J. Z.; Nie, S. *Nat. Biotechnol.* **2001**, *19*, 631.

(3) (a) Wu, C. L.; Zheng, J. S; Huang, C. B.; Lai, J. P.; Li, S. Y.; Chen, C.; Zhao, Y. B. *Angew. Chem., Int. Ed.* **2007**, *46*, 5393. (b) Gao, X. H.; Nie, S. M. *Anal. Chem.* **2004**, *76*, 2406. (c) Qian, X. M.; Nie, S. M. *Chem. Soc. Rev.* **2008**, *37*, 912. (d) Chen, Z.; Tabakman, S. M.; Goodwin, A. P.; Kattah, M. G.; Daranciang, D.; Wang, X. R.; Zhang, G. Y.; Li, X. L.; Liu, Z.; Utz, P. J.; Jiang, K. L.; Fan, S. S.; Dai, H. J. *Nat. Biotechnol.* **2008**, *26*, 1285. (e) Cao, Y. C.; Jin, R. C.; Nam, J. M.; Thaxton, C. S.; Mirkin, C. A. *J. Am. Chem. Soc.* **2003**, *125*, 14676.

(4) (a) Zhao, Y.; Shum, H. C.; Chen, H.; Adams, L. L. A.; Gu, Z.; Weitz, D. A. *J. Am. Chem. Soc.* **2011**, *133*, 8790. (b) Giri, S.; Sykes, E. A.; Jennings, T. L.; Chan, W. C. W. *ACS Nano* **2011**, *5*, 1580.

(5) Finkel, N. H.; Lou, X. H.; Wang, C. Y.; He, L. *Anal. Chem.* **2004**, *76*, 353A.

(6) Wang, G. F.; Park, H.-Y.; Lipert, R. J. *Anal. Chem.* **2009**, *81*, 9643.

(7) (a) Sahoo, S.; Husale, S.; Karna, S.; Nayak, S. K.; Ajayan, P. M. *J. Am. Chem. Soc.* **2011**, *133*, 4005. (b) Howes, P.; Green, M.; Bowers, A.; Parker, D.; Varma, G.; Kallumadil, M.; Hughes, M.; Warley, A.; Brain, A.; Botnar, R. *J. Am. Chem. Soc.* **2010**, *132*, 9833. (c) Castle, A. B.; Gracia-Espino, E.; Nieto-Delgado, C.; Terrones, H.; Terrones, M.; Hussain, S. *ACS Nano* **2011**, *5*, 2458.

(8) (a) Cui, Y.; Zheng, X. S.; Ren, B.; Wang, R.; Zhang, J.; Xia, N. S.; Tian, Z. Q. *Chem. Sci.* **2011**, *2*, 1463. (b) Wang, Z. Y.; Zong, S. F.; Yang, J.; Li, J.; Cui, Y. P. *Biosens. Bioelectron.* **2011**, *26*, 2883.

(9) Wang, Z. Y.; Wu, H.; Wang, C. L.; Xu, S. H.; Cui, Y. P. *J. Mater. Chem.* **2011**, *21*, 4307.

(10) Xiang, Y. J.; Wu, X. C.; Liu, D. F.; Li, Z. Y.; Chu, W. G.; Feng, L. L.; Zhang, K.; Zhou, W. Y.; Xie, S. S. *Langmuir* **2008**, *24*, 3465.

(11) (a) Wang, L.; Tan, W. *Nano Lett.* **2006**, *6*, 84. (b) Blaaderen, A. V.; Vrij, A. *Langmuir* **1992**, *8*, 2921.

(12) (a) Wang, G. F.; Lipert, R. J.; Jain, M.; Kaur, S.; Chakraboty, S.; Torres, M. P.; Batra, S. K.; Brand, R. E.; Porter, M. D. *Anal. Chem.* **2011**, *83*, 2554. (b) Bishnoi, S. W.; Lin, Y. J.; Tibudan, M.; Huang, Y.; Nakaema, M.; Swarup, V.; Keiderling, T. A. *Anal. Chem.* **2011**, *83*, 4053.